Experimental Study of an Acoustically Excited Plane Jet at Low Reynolds Numbers

S. Marzouk† and N. Hnaien

National Engineering School of Monastir, Unite of Metrology and Energy Systems, 5000 Rue Ibn Jazzar, Monastir 5035 Monastir, Tunisia

†*Corresponding Author Email: saloua.marzouk@issatgb.rnu.tn*

ABSTRACT

The dynamics of a vertical two-dimensional air jet under acoustic excitations at a low Reynolds number are investigated experimentally. The perturbation is introduced by means of a loudspeaker located in a settling chamber before the nozzle exit. The experiments are operated at Strouhal number St ranging from 0 to 1 and for different pulsation amplitudes. A laser plan is used to visualize the flow and the hot-wire anemometry for more specific measures of the mean and fluctuation velocity. The discussion is focused on the influence of two parameters governing the flow: the Strouhal number St and pulsing amplitude. The main results show that the flow consisting of the vortex propagating downstream a nozzle exit is strongly affected by the excitation. Indeed, the introduction of an external perturbation introduces a more rapid degeneration of the potential core with the appearance of vortices near the nozzle as the pulsation amplitude increases. These vortices are amplified and become larger than the nozzle width which induces the enhancing of the entrainment and mixing effects of the shear layers. Another very important phenomenon is observed: the excitation has led to the formation of a switching from the asymmetric mode (sinuous mode) to the symmetric mode (varicose mode).

Keywords: Two-dimensional jet; Pulsating amplitude; Frequency; Flow visualization; Hot-wire anemometer.

NOMENCLATURE

A	dimensionless pulsating amplitude	u'	streamwise turbulent fluctuation
e	nozzle width	x, y	cartesian coordinates
f	frequency of excitation	ν	viscosity of fluid
Re	Reynolds number		
St	Strouhal number	**Subscripts**	
t	time	0	at nozzle exit
T	period of excitation		
U	mean streamwise velocity		

1. INTRODUCTION

One of the most interesting properties of the jets is their ability to mix with the ambient fluid. Several attempts have been made to improve the mixing jets rate by the means of vortices generated and/or artificially intensified. The improvement of the mixing process has witnessed considerable interest in both fundamental and industrial aspects. As far as the fundamental aspect, it has been widely suggested that the mixing process is closely related to the turbulence transition (see Dimotakis (2000), Hinze (1987)) and the nozzle geometry as well as the initial perturbations strongly influence its generation and transition (see Hussain and Husain (1989), Crow and Champagne (1971)). For practicality, there are many. The mixing process conditions, the propulsion force of the aircraft engines, the efficiency of combustion in the mixing chambers, the pollutants dispersion in industrial sites and finally, in the habitable spaces, the amount of the air diffused and therefore the thermal comfort of the users.

The dynamics of pulsed jets has generated great interest in the scientific community since Crow and Champagne (1971) have studied the ordered vortex structure in the potential core region of circular turbulent jets at a Reynolds number equal $Re = 10^5$. They found at a downstream location of four

diameters, an increase in the entrained volume flow of 32% at Strouhal number ($St = f\,e/U_0$, where f is the frequency of excitation, e is the nozzle width and U_0 is the exit streamwise velocity) of 0.3 and at small pulsing amplitude of 2% over a corresponding steady jet.

Several experiments on the jet under acoustic excitations are investigated in the potential core area by Binder *et al.* (1973), Rockwell (1972), Kibens (1980), Zaman and Hussain (1980), Hussain and Zaman (1980). Their results suggest that the excitation strongly affect the initial region and is manifested by an increase in the size of the coherent structures. Some works have also used an acoustic excitation as a tool to artificially increase the size of the vortex structures to study them.

The effects of a controlled excitation on the mean and temporal quantities in the nozzle vicinity of the plane jet were treated by many researchers (see e.g. Rockwell (1972), Hussain and Thompson (1980), Ho and Huang (1982), Thompson (1975), Sato (1960), Goldschmidt and Kaiser (1971)). The results are significantly different from those observed in the axisymmetric jets studied by Crow and Champagne (1971), Zaman (1978); Zaman and Hussain (1980). The size, training and nature of interactions between the coherent structures in the nozzle near area are different in the two jets types. Industrial applications suggest the use of excited elliptic jets to promote the mixing and control of aerodynamic noise. In this context, Husain and Hussain (1983) were interested in the study of an elliptical jet under a sinusoidal excitation controlled by a loudspeaker. At the fixed pulsation amplitude of 2%, they found an increase of 150% and 190% of the turbulent intensity in a cross section. This increase is significantly larger than that for a circular jet Hussain and Zaman (1980) and as that obtained with a whistler nozzle that is studied by Hasan and Hussain (1982). Farrington and Claunch (1994) carried out the visualization by a full-field infrared imaging to determine the pulsation influence on a plane jet behaviour and mixing. The results are obtained for a Reynolds number equal to Re=7200 and a Strouhal number range between 0 and 0.324. They noticed that for pulsating jets, the vortices are larger than the steady jet and occurred in the nozzle vicinity. The formation of large, periodic vortices by large-amplitude pulsations increases the mixing and spreading of the jet. The model of the irregular vortices obtained with a non-pulsed jet is transformed by pulsation to two trains of vortices which are better organized and periodic and symmetrical with respect to the nozzle axis. They showed that jets pulsed with a high pulsing amplitude entrained surrounding fluid more quickly than steady jets.

Marzouk *et al.* (2015) studied numerically by modeling with large Reynolds numbers the influence of an initial perturbation on the spatial and temporal evolutions of the dynamic and thermal quantities of a plane jet in turbulent regime. These authors found that the pulsation considerably affects the flow in a region close to the nozzle and then reach an asymptotic regime identical to that of a non-pulsed jet. They also revealed that the pulsation considerably accelerates the expansion of the jet and significantly improves the diffusion and entrainment as well as the heat exchange with the surrounding environment in the first diameters.

Andersen *et al.* (2016) investigated numerically and experimentally the cleaning of low pressure fabric filters (2 bars) by pulsed jet. They showed that the 3D unsteady RANS simulation is ideal to optimize the design of the cleaning system in fabric filters with pulse jet. They noticed that the pulsed jet has a highly transient behaviour whilst cleaning. In addition, during the subsonic ramp-up of the jet, they observed large instabilities in the shear layer between the jet and the surrounding stagnant environment, resulting in the formation of several compressible vortex rings.

A detailed study of the response of a turbulent plane jet to acoustic excitation is accomplished by Chambers (1977) and Chambers and Goldschmidt (1982). They indicated that the acoustic pulsation of a wide frequency range produces changes in the mean flow structure. They also found that for some frequencies the turbulent intensity and the Reynolds stress increased in the jet main area while the acoustic excitation effect decreases downstream. They concluded that the interaction origin of an acoustic disturbance with the jet is observed in the shear layers of the nozzle vicinity. Thomas and Goldschmidt (1981) experimentally studied the influence of acoustic excitation on the plane jet. They showed that the expansion rate is larger for an excitation at Strouhal numbers of 0.34 and 0.42. This is in good agreement with those reported by Goldschmidt and Kaiser (1971) at Strouhal number equal to 0.42 and by Chambers and Goldschmidt (1981) for a Strouhal number equal to 0.38. However, the increases noted by Thomas and Goldschmidt (1981) are generally for large amplitudes. They also found that the expansion rate increases are accompanied by increases in turbulent intensities for different Strouhal numbers.

Hussain and Thompson (1980) experimentally studied the influence of a sinusoidal disturbance on the air plane jet. They proved that the excitation influence, on the fields of the mean and fluctuating velocity is much lower than in the case of circular jet established by Zaman and Hussain (1980) and Hussain and Zaman (1980). They found that the growth rate is much larger and the wavelength is much smaller in the shear layer than on the jet axis. The wave reaches its maximum amplitude at St=0.18 on the jet axis, and at St=0.45 in the shear layer. The growth rates and the wave numbers distributions increase with Strouhal number in the shear layer and on the jet axis but tend to approach to constant values to larger Strouhal numbers. The induced symmetric mode remains symmetric as it travels downstream, while the plane jet acts as a non-dispersive waveguide at low Strouhal number.

Recently Lio *et al.* (2013) experimentally studied the dynamics of the flapping motion of a

rectangular jet subjected to acoustic excitation by means of the hot-wire measurement and the flow visualization with the smoke method. They showed that the excitation frequency has significant effects on the jet flapping. As the excitation frequency is high, the position where the vortex begins to appear becomes upstream, and the streamwise interval between vortices becomes shorted, and then the vortex size becomes small.

Although in previous studies, the excited jet propagation at a large Reynolds number is shown by the measurements of a mean axial-centerline velocity, aggregate turbulence intensity along the centerline, dynamic half-thickness of the jet and the boundary layer thickness must be affected by excitations.

The visualization results are not sufficient to understand the propagation mechanism of the vortices structures and also the pulsation merger downstream. In addition, various researches are devoted to the Strouhal number effect at fixed pulsation amplitude. As is known the pulsation is characterized by two parameters which are the frequency and the amplitude. In this context, this study aims to visualize the vortices structures in two-dimensional jet with different external excitations by means of smoke wire technique and high speed camera. Much attention was paid to discuss the effects of external excitation on formation of coherent structures and their propagation mechanism in laminar regime.

2. EXPERIMENTAL STUDY

2.1 Experimental Setup:

Figure 1 shows schematically the experimental arrangement. It comprises the flow generator (the nozzle and accessories), the lighting device (laser and shaping optics), and the shooting system (camera).
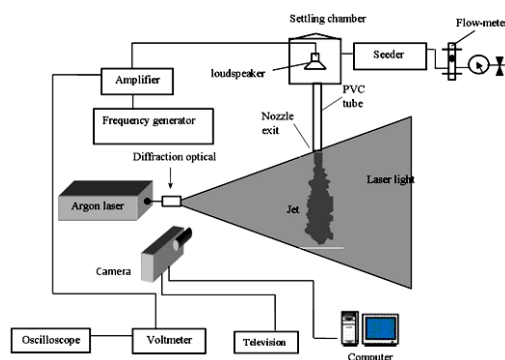

Fig. 1. Experimental setup.

The jet issuing vertically downward from a rectangular nozzle supplied with air at constant temperature from an air compressor. Thereafter, it passes through two flowmeters, one for measuring the low flow rates and one for high flow rates. These flow meters are connected to a manometer for adjusting the circulating air pressure. We have

given the error related to the flowmeter (10% of the maximum height of the ball) to which must be added the read error (±1mm). Air is, then, seeded with approximately 1 μm diameter glycerin particles (seeding density ≈ 30 particle ml^{-1} of pure jet fluid) used as a tracer.

The disturbance mechanism was dictated by observations made during the literature review. The acoustic excitation system consists of a function generator, an amplifier and a loudspeaker, as shown in Fig. 1. A sinusoidal excitation from a low frequency generator, after being amplified, was used to drive the loudspeaker. The latter is attached to the inside a plenum chamber and aligned with the jet axis for periodic forcing of the flow. In the system, the forcing frequency is determined by adjusting the function generator and/or the amplifier.

A voltmeter and an oscilloscope are placed between the amplifier and the loudspeaker respectively to measure the electrical signal amplitude and check that it does not saturate the output of the amplifier Fig. 1. We chose to conduct the experiments for Strouhal numbers between 0 and 1 that seem most interesting from the bibliographic, while the pulsing amplitude is chosen between 0 and 25% of the ejection velocity. The used nozzle is fixed at the end of a PVC tube of a length 50cm. This tube is fixed vertically at settling chamber and long enough to allow a flow established at the nozzle exit. To obtain a two-dimensional plane jet, the tube is equipped with a rectangular nozzle of is 6mm thick, 64mm wide and with an aspect ratio (thickness to width ratio) equal to 11.

2.2 Flow visualization

Flow visualization is performed to provide qualitative information about the effect of the acoustic excitation on the formation of coherent structures along the jet.

Visualizations are made by laser anemometer, which is a method of non-intrusive optical investigation: it provides instant jet visualization. A 1.2W continuous Argon Ion laser class IV emitting green radiation of wavelength 523 nm was used as the light source. A spectra-physics Argon-Ion laser coupled with a beam-steering optics and a cylindrical lens provided the light sheet to illuminate the flow field plan. This plan, at high contrast, determines the sharpness of images filmed by a high-speed digital CCD video camera (shutter velocity from 1/50 to 1/10000 second) aligned perpendicular to the jet axis and connected to a television for observing the flow in real time. A workstation connected to the video camera (Sony model CCD V 6000 E, 25 frames per second) allows, thanks to an integrated software (LABVIEW 2), to process images. This device allows in particular selecting instantaneous images or integrated over time.

2.3 Hot-Wire Anemometer

The hot wire anemometer is a technique frequently used for the experimental study of gas flow. In our

experiments, we used the hot wire anemometry system with DISA 55M01 main unit, DISA 55M10 CTA standard bridge, and the power supply 55M05.

Velocity measurements were performed using metal hot-wire probe (consists of a sensitive tungsten wire). All probes used in experiments had a diameter of 4 μm and a length of 0.6254mm. This wire is heated by Joule effect to a temperature of 200°C and immersed in the air jet at a temperature around 20°C. The temperature of the sensitive element of the probe is kept constant by a servo electronics system. The heating current intensity is related to the cooling caused by the fluid flow velocity in contact with the probe. The voltage measurement across the sensitive element can determine the flow velocity recorded by the probe. The hot wire is calibrated by a Pitot tube placed in the test section of a convergent wind tunnel. The calibration curve was computed using King's law. The traversing of the probe was controlled by a very accurate computer via 16 bit A/D converter. After, the data were analyzed with a data-processing computer system.

The single hot wire probe was perpendicularly located with the pulsed jet flow at the nozzle exit center where the mean axial velocity is maximal.

Our main concern in using the hot wire was to quantify the perturbation magnitude introduced by the loudspeaker. Indeed, the setting of this parameter posed a problem considering the non-linearity between the response curves of the amplifier and the loudspeaker. So, we used the hot wire to quantify the perturbation by spotting versus the fluctuation percentage of the ejection velocity.

We worked with a fast acquisition frequency of 50 kHz; this reduces our pulse frequency range of jet to 25000 Hz in accordance with the Shannon criterion which requires the acquisition frequency that is the double of the studied phenomenon frequency.

Before each acquisition, we defined a sufficient point number n in order to obtain a good accuracy in velocity measurement. The point number n and the acquisition frequency f_a will characterize sampling time defined by: $T_e = n/f_a$.

By means of the usual Reynolds decomposition, the instantaneous streamwise velocity of the pulsed jet U_i can be expressed in terms of a mean axial velocity U and the aggregate axial turbulence u as $U_i = U + u$

We have access, through a computer with a recording software and data processing, to the mean axial velocity determined from a discrete equation over a finite time period as in $U = \sum_{i=1}^{n} U_i / n$, where

U_i is the ith sampled signal, n is the total number sampled.

Under a sufficiently large number of samples in a digital sampling process, the standard deviation is

also described, which is written as: $\sigma = \sqrt{\overline{u^2}}$. The turbulence intensity I is given as: $I = \sigma/U = u'/U$. In this work, all velocity component terms refer to the velocity components along the centerline jet.

The jet visualizations and the velocity measurements were performed under the various conditions of the Reynolds number, pulsation frequency (Strouhal number) and pulsation amplitude a summarized in Table 1.

Table 1 Experimental characteristics of the jet

e, mm	St	Re	U_0, m/s	a, m/s
6	0.1- 1	500	1.45	0.072; 0.145; 0.36
		1200	3.14	0.16; 0.31; 0.78

3. RESULTS AND DISCUSSION

The visualization of excited and non-exited two-dimensional jet was performed to study the influence of acoustic excitation on the vortex structures involved in the flow. A wide range of the Reynolds number is explored to identify their influence on the jet behavior. However, in this work, we chose only two Reynolds numbers that are *Re*=500, and *Re*=1200 which correspond to velocity at the origin which was set equal to $U_0 \approx 1.45$ m/s and $U_0 \approx 3.14$ m/s.

The coordinate's origin O is fixed at the nozzle center. The coordinate system is Cartesian one with streamwise component *x*-axis and the *y*-axis in the horizontal direction perpendicular to the flow (Fig. 2).

3.1 Quantification of the Jet Exit

xOne of the objectives of the hot-wire study is to characterize the velocity time evolution at the nozzle exit as a function of the excitation.
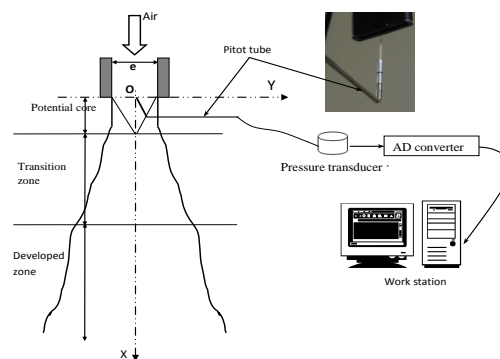

Fig. 2. Experimental setup of measurement.

Measurements are performed directly at the nozzle center (Fig. 2) and in the variation range of the frequency and pulsation amplitude. The disturbance amplitude is determined by the standard deviation of the streamwise velocity at the nozzle exit center.
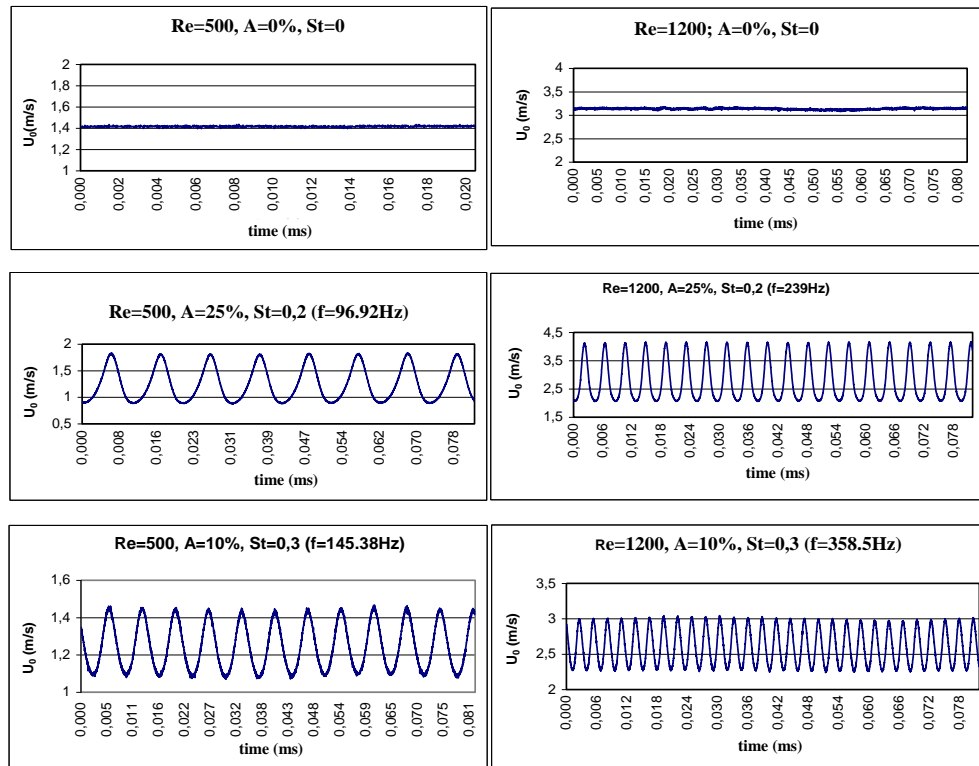
Fig. 3. Temporal evolution of axial velocity at center of nozzle exit for different Strouhal number and pulsation amplitude.

The temporal signal of the velocity is measured to check that the jet excited at imposed frequency and amplitude Figure 3 shows the temporal evolution of the centerline velocity at the nozzle exit as a function of the excitation and for two Reynolds numbers. We can conclude from these velocity curves (sinusoidal) on how the perturbation is transmitted to the jet. The effect of the perturbation introduction

3.2 Visualization of Non-Pulsed and Pulsed Jets

Figure 4 illustrates the instantaneous flow visualization of the plane jet flow for a small pulsation amplitude equal to 5% and for two low Reynolds numbers 500 and 1200.

Figure 4a and Fig. 4d show the photographing images of non-pulsed jet in which several vortex structures may be identified downstream from the nozzle.

These images show the existence of three distinct zones in the jet propagation. The first jet region is characterized by a short laminar zone, called the potential core region, followed by a region of a very low ripple (region I). In this zone the centerline velocity remains constant and equal to velocity at the nozzle exit. The potential core represents the

in the flow is manifested by a near-perfect sinusoidal variation of the instantaneous velocity: Thus we conclude that the acoustic excitation

imposed to the jet by the loudspeaker positioned upstream in the settling chamber is transmitted at the nozzle exit without deformation. Note that the velocity signal is perfectly sinusoidal, indicating that the acoustic excitation produces a sinusoidal perturbation of the nozzle mass flow. Consequently; the instantaneous velocity profile at the nozzle exit may be periodically modulated by the following equation: $U_{C0} = U_0 \left(1 + A \sin \left(2\pi f t\right)\right)$ where U_0 is the mean velocity profile of the non-pulsed jet, A is dimensionless pulsation amplitude ($A = a/U_0$) and f is the frequency inner boundary of the structures that develop on the jet surface (Crow and Champagne (1971)).

The second region represents a transition region wherein the centerline velocity decreases. The Kelvin-Helmholtz instabilities that develop flow downstream in the shear flow are observed in this region (region II). These instabilities are characterized by the winding vortex ring which is due to a depression inside the vortex thereby causing aspiration of the external environment fluid. Finally, these vortices finish in a chaos and disorder area where disappear completely after $x/e > 8$ (region III).

In general, the development of a two-dimensional jet is initially in varicose mode, and switches to a sinuous mode near the end of the potential core (Iio *et al.* (2010)). For all visualizations carried out for
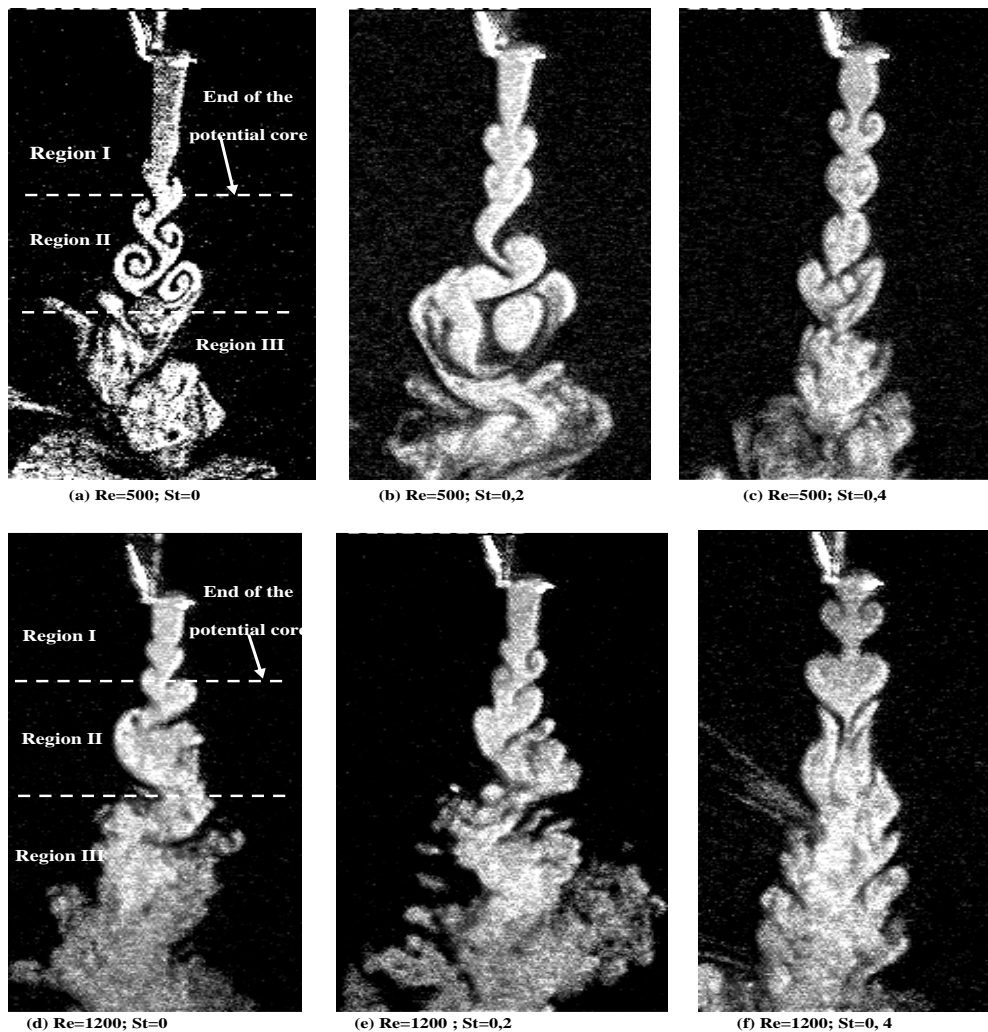
Fig. 4. Instantaneous flow visualization of plane jet for two low Reynolds numbers at pulsation amplitude A=5%.

the non-pulsed plane jet, it is observed that the initial roll-up vortices develop varicose mode and switches to sinuous mode near the end of the potential core for Reynolds number *Re*=1200 (Fig. 4d), while for Re=500 (Fig. 4a), the morphology of the jet is entirely different. Note that the jet flow remains unstable and this instability is still Kelvin-Helmholtz instability with an axisymmetric mode (sinuous mode). It is observed that the instability mode depends on the jet exit velocity or of the Reynolds number.

In the near field of rectangular jets, large scale coherent structures are detected and examined by a number researcher. Both symmetric and axisymmetric modes of instabilities were identified in the initial shear layer region. The mode type depends on the profile shape of the velocity at the exit of the rectangular jet (Goldschmidt and Kaiser (1971)), the Reynolds number (Yeh *et al.* (2009)), the position downstream (Yeh *et al.* (2009)) and the nozzle geometric configuration ejection such as that the ratio of width by the thickness of the nozzle (Yeh *et al*. (2009) and Hasio *et al.* (2010)).

For a non-pulsed jet, the flow remains parallel to the jet axis and slightly flared and the length of the potential core area decreases as the Reynolds number increases and no coherent structures are observed in the near field (Fig. 4a and Fig. 4d).

There is also a loss of the organized character of the flow, the turbulence zone (region III) becomes more critical as the Reynolds number increases, which confirms the importance of this parameter on the jet behavior. At a low pulsation amplitude equal to 5% and for a Strouhal number equal to St =0.4, Fig. 4c (for Re=500) and Fig. 4f (for Re=1200) show that the flow has a succession of symmetrical swelling and converging relative to the jet center in a varicose mode. These instability waves are increasingly near the ejection nozzle when the Reynolds number increases.

While for a Strouhal number St=0.2 and for a Reynolds number Re= 500 (Fig. 4b), the development of a two-dimensional jet is initially in a varicose mode and changes to a sinuous mode whereas for a Reynolds number equal to Re= 1200 and for a Strouhal number equal to St=0.2 (Fig. 4e), the flow presents a rhythmic and asymmetric undulation relative to the center line (phenomenon
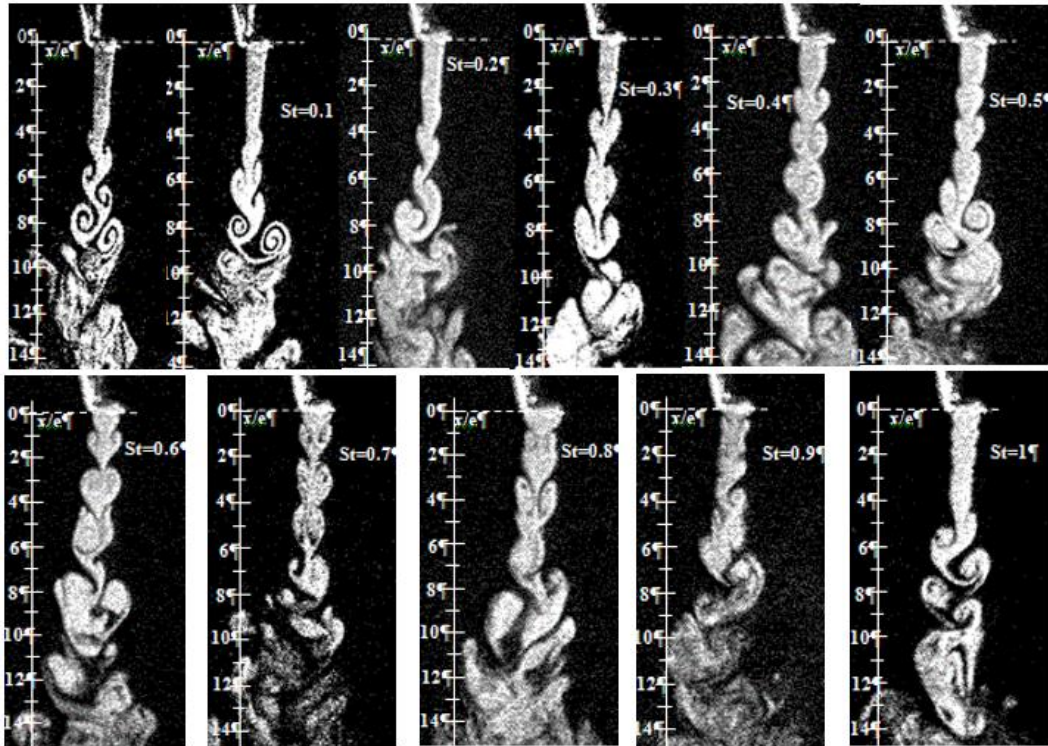
Fig. 5. Instantaneous flow visualization of plane jet for different Strouhal numbers at Re=500 and A =5%.

of the jet flapping). Thus, the instability waves are performed in a sinuous mode. It is clear that some eddies appear to be symmetric and asymmetric relative to the jet axis. Then, both instability modes (sinuous and varicose) also exist for a two-dimensional jet subjected to acoustic excitation. The existence of these modes of instability depends on the Reynolds and Strouhal numbers.

In addition, the interaction between the right and left vortices causes the phenomenon of the jet flapping that appears after the potential core (zone II) whose magnitude is greater than the nozzle exit width. It is closely in agreement with the results of Yeh *et al.* (2010). Goldschmidt *et al.* (1983) suggested that the flapping motion amplitude is slightly greater than the nozzle exit width and its movement is directly related to the asymmetric arrangements of vortices. The symmetric vortices decompose to smaller eddies beyond x/e=8.

Figure 5 reports the comparison of the qualitative behavior of the isothermal jet, pulsed for different Strouhal numbers at a low pulsation amplitude (A= 5%) obtained by instant viewing by the laser plane. A typical vortex formation in the non-pulsed jet is shown (for St=0). When the jet is excited at St=0.3 a symmetric alignment of vortices which is known as the varicose mode, is clearly observed. The excitation led to the formation of a switching from the asymmetric mode to the symmetric mode. The two instability modes exist along the pulsed jet evolution. Indeed, for lower frequencies ($0<St\leq0.2$), the asymmetric structures occur. As the forcing frequency is increased ($St\geq0.3$), large symmetric structures exist.

The same image allows us to note that for the Strouhal numbers range $0.6\leq St<1$, the jet flow field demonstrates the existence of two distinct regions. The length of pulse is dominated and the high turbulence steady jet region depends on the imposed pulsating frequency and amplitude.

This is in good agreement with previous results established by Hariyo and Bremhorst (2012). But Hussain and Thompson (1980) studied the near field of a plane jet submitted to sinusoidal acoustic disturbances. They found that the induced symmetric modes remain symmetrical because they propagate downstream.

Figure 5 also shows that the roll vortex of the unexcited jet is clearly observed that beyond $x/e\approx6$, while even at a low Strouhal (St=0.1 which corresponds to a pulse frequency equal to 48.45 Hz), the vortices are clearly observed after $x/e\approx6$.

When the jet is excited at St=0.3, the symmetrical alignment of vortices, known as the varicose mode is clearly observed. Indeed, the excitation leads to the formation of a switching from the asymmetric mode to the symmetric mode. The vortex size is larger than those occurring in the unexcited jet. The vortex winding position is approximately at $x/e\approx 3$, and the distance between eddies in the flow is less than the unexcited jet.

Another key point revealed in the pulse dominated region; the pulsed jet potential core completely disappear under the disturbance effect. Indeed for St=1, we see the appearance of the column mode just at the nozzle exit vicinity which extends over a distance close to $x/e\approx5$, with a strengthening of
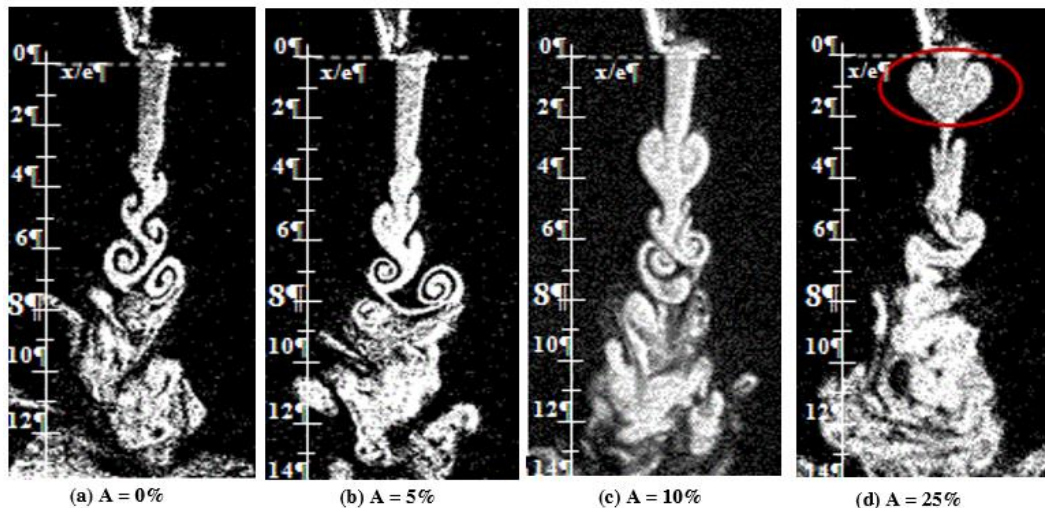
Fig. 6. Pulsation amplitude effect on the jet evolution for Re = 500, and St = 0.1.

(a) A = 0%   (b) A = 5%   (c) A = 10%   (d) A = 25%
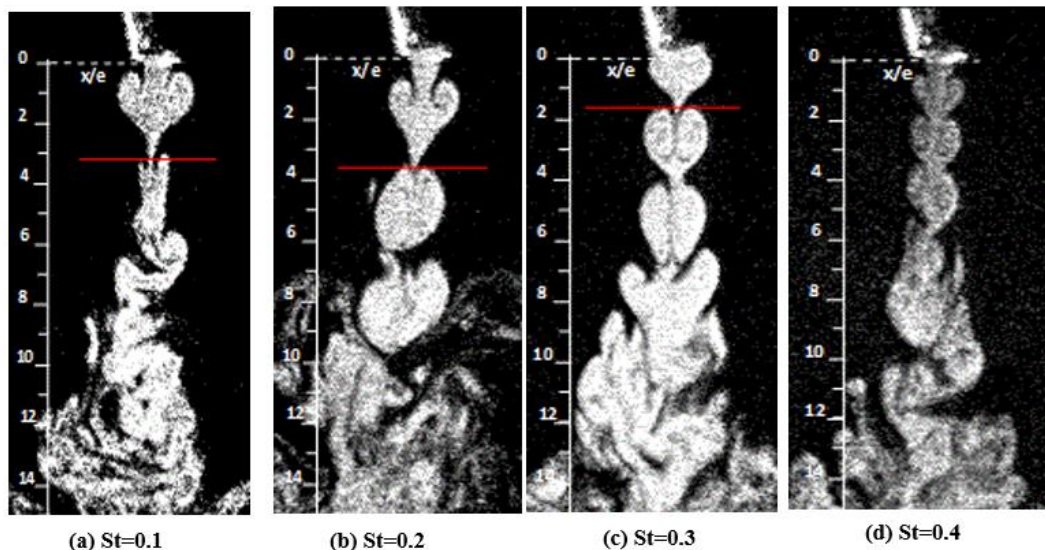

(a) St=0.1   (b) St=0.2   (c) St=0.3   (d) St=0.4

Fig. 7. Instantaneous flow visualization of jet for different Strouhal numbers at Re=500 and A =25%.

vortex pairs. So, the pulsed jet structures at a high Strouhal number St=1 are radically different from the non-pulsed jet. Beyond $x/e\approx4$, the rolling movement of vortices resulted in the surrounding fluid advantage to increase the mixture.

In this study, the excitation at a low pulsation amplitude (A=5%) and low Strouhal number reveals the primary influences. Indeed, the structures of the pulsed jet are similar to the non-pulsed jet ones in pulsed jet are similar to the non-pulsed jet ones in the potential core region. The length of the potential core decreases due to the vortex structures occurrence increasingly the nozzle vicinity when the Strouhal number increases. Crow and Champagne (1971), Goldschmidt *et al.* (1983) and Lovett and Turns (1990) show that the excited jet becomes less dispersive at a high pulsing frequency. This contradicts what is revealed by Binder *et al.* (1973), Bremhorst and Harch (1979) and Tanaka (1984), but it is in agreement with our findings. Indeed, the pulsed jet is less dispersive in the potential core area at a high pulsing frequency (St=1

corresponds to a pulse frequency equal to 485 Hz). The flow develops like a non-pulsed jet with a fragmentation of the vortex structures in the fully developed turbulence region.

To study the influence of the pulsing amplitude on the jet development, we present in Fig. 6, the visualization of an excited jet for different pulsing amplitudes and at a low Strouhal number (St = 0.1).A decrease of the potential core length is observed with the formation of a vortex pair increasingly at the nozzle vicinity when the pulsation amplitude increased. These vortices are amplified and become larger than the nozzle exit width when the pulsation amplitude increases.

These large vortices produce an increase of the external fluid entrainment and lead to a jet widening right out the nozzle exit with a decrease in the centerline mean velocity (Fig. 8 and Fig. 9). For large pulsation amplitudes, the excitation jet entrains the surrounding fluid to occur more rapidly and decreases faster than the non-pulsed jet (Farrington and Claunch (1994)).

It is interesting to note that at a large pulsation amplitude (Fig. 6d), the flow presents a single vortex at the nozzle vicinity whose width (length scale) is twice the nozzle width. This vortex (inside the red ellipse) is detached from the main flow at approximately $x/e \approx 3$. This phenomenon is very interesting and leads us to present in Fig. 7, the instantaneous visualizations of the pulsed jet for different Strouhal numbers and at a high pulsing amplitude equal to A=25%. We see, then that the potential core is completely absent for different consider Strouhal numbers. We also note the presence of a symmetric vortex structure in the nozzle exit moving downstream of the jet.

At St=0.4, large vortices with a length scale slightly greater than the nozzle width appear in the region close to the jet exit ($0.5 \leq x/e \leq 2$); while at $St \leq 0.3$ the eddies length scale is greater than nozzle width.

From Fig. 7a, we also observe that at a low Strouhal number equal to St=0.1, the formation of a single vortex in the nozzle vicinity and its width is greater than the nozzle one. The number of vortex pairs increases with the Strouhal number (indeed at St=0.1 there is one vortex pair, while at St=0.3 there are two vortex pairs and at St=0.4 there are three vortex pairs which propagate on the varicose mode in the downstream).

On the other hand, the formation of the vortex structures with a large scale is clearly observed and proves to be much larger in the case of the Strouhal number $St \leq 0.3$ (Fig. 7b) than in the case of the Strouhal number equal to St =0.4. Another interesting observation is that the potential core

region is completely gummed for the large pulsation amplitudes (A= 25%) and even at a low Strouhal number.

Indeed, the conducted visualizations show that the imposed pulsation significantly affects the flow jet field associated with the existence of two distinct regions. In addition, the length of each area strongly depends on the variation of the frequency and pulsing amplitude. These results can justify the decrease in the axial velocity right out of the nozzle represented thereafter.

3.2 Velocity and Turbulence Intensity Measurements Pulsed Jets

Figure 8 shows comparisons of longitudinal evolution (where x/e is the nondimensional longitudinal coordinate) of the decay of the inverse of square of the mean centerline axial velocity characterized by the dimensionless parameter $(U_0/U_c)^2$ between the existing results of the pulsed and steady jets.

From the figure, it can be seen that the centerline longitudinal velocities are constant in the potential core area, near the jet exit $x/e \leq 3$, and equal to the centerline exit velocity.

In this region, our results are in perfect agreement with the experimental results of Yeh *et al.* (2009) and Stamatios and Ellen (2001), in addition, the

pulsation has no effect on this parameter and the flow behaves as a non-pulsed jet

Similar patterns of the decay of centerline longitudinal velocity as illustrated in Fig. 8 appear among the pulsed and steady jets researchers (Yeh *et al.* (2009) and Stamatios and Ellen (2001) and the present researcher). This parameter increases with the longitudinal distance, as has been well documented in the literature. In the self-similar region defined for ($x/e > 3$), a difference between our results and the results of Yeh *et al.* (2009) and and Stamatios and Ellen (2001) is observed. This is due essentially to a different Reynolds number and pulsing frequency and amplitude used.

At St=0.3, the centerline velocity decay is slightly greater than that for a non-pulsed jet for $3 \leq x/e \leq 5$. At $x/e = 6$, the two curves intersect followed by a deceleration of the centerline velocity decay further downstream. However, the centerline velocity decay tends to be closer that observed in the non-pulsed case when the Strouhal number increases (St=0.9) as soon the nozzle.
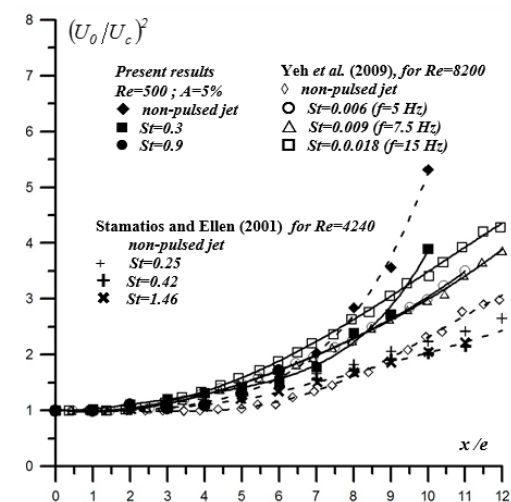

Fig. 8. Longitudinal evolution of the decay of inverse of square of the mean centerline axial velocity.

The effect of the pulsing amplitude on the centerline velocity decay is shown in Fig. 9 for a Reynolds number equal to Re=500, by increasing the pulsation amplitude at 10%, we note that the profiles of the centerline velocity decay are almost confused with the jet pulsed at 5%. A difference is noted only for the Strouhal number equal to 0.3 and from $x/e \geq 5$ where the velocity decreases slowly at a low pulsation amplitude (A=5%).

In order to study the phenomena of the turbulence enhancement and suppression in the flow, we represent, on Fig. 10 and Fig. 11, the longitudinal distribution of the normalized centerline turbulence intensity at two pulsation amplitude 5% (Fig. 10) and 10% (Fig. 11).

The centerline turbulence intensity u_c'/U_0 of the non-pulsed jet has the characteristics of the

distribution of a jet exiting a classical rectangular nozzle (low level of turbulence in the potential core).
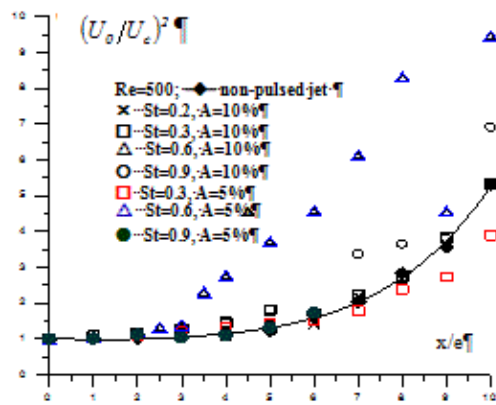

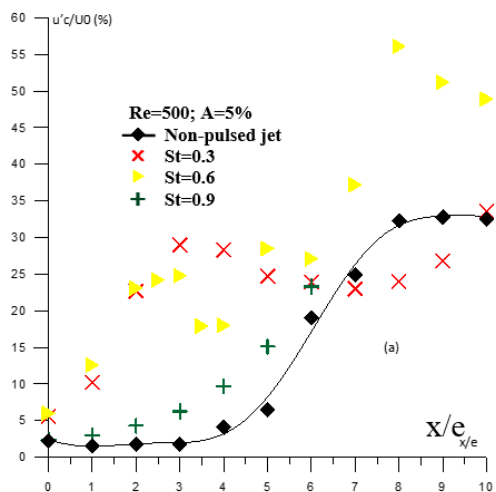**Fig. 9. Longitudinal evolution of centerline velocity decay normalized.**

Fig. 10. Longitudinal evolution of the centerline turbulence intensity normalized for A=5%.

After a low value equal to 0.02 at the nozzle exit, the centerline turbulence intensity increases monotonically along the axial distance and begins to stabilize near $x/e = 8$ where it reaches a maximum value of about 0.32. Heskestad (1965) and Sfeir (1979) reported values of 0.25 in the self-similar region of their jets and Stamatios and Ellen (2001) reported value of 0.2 near $x/e = 10$.

Pulsed at $St = 0.3$ and at a low pulsation amplitude 5% (Fig. 10), causes an improvement in the turbulence intensity in the near field of the nozzle ($0 \le x/e < 7$) while a decrease of this parameter occurs beyond $x/e \ge 7$ then, back an improvement noted at $x/e = 10$. However, at a pulsation amplitude $A=10\%$ and St=0.3, the turbulence intensity increases until reaching a maximum of value about 0.28 near $x/e = 4$. Beyond this distance, it decreases until a minimum value at $x/e = 7$ before increasing again.

In addition, the decrease in the centerline turbulence

intensity along the axial distance is obvious, because of the significant deceleration of the centerline velocity, when pulsed at St=0.6, it causes a strong increase in the turbulence intensity at the nozzle exit for the two considered pulsations amplitudes. The high values of the turbulence intensity, obtained in our experiments are probably due to the turbulence intensity calculated without removing the component of the sinusoidal variation from the instantaneous velocity measured directly.
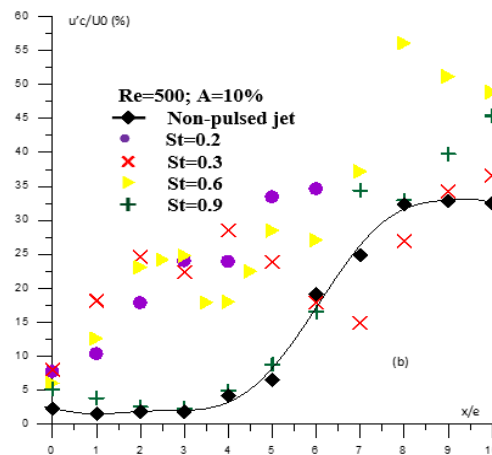

Fig. 11. Longitudinal evolution of the centerline turbulence intensity normalized for A=10%.

A significant decrease of the centerline velocity corresponds to an increase of the turbulence intensity at a low axial distance. This may lead to the conclusion that the mixing and diffusion of the jet is improved by the pulsations which occur in the near field of the nozzle.

4. CONCLUSION

The research activity presented in this document is a contribution to the experimental study of an air jet ejected from a rectangular nozzle at a low Reynolds number (*Re*=500 and *Re*=1200) submitted to an acoustic excitation.

The hot wire anemometer used allowed us to determine and ensure that the acoustic excitation transmitted to the nozzle exit and the centerline velocity profile at the nozzle exit is sinusoidal.

Visualizations carried out allowed us to deduce that the phenomena of the formation and deformation of vortex structures are strongly affected by the excitation.

Indeed, the excitation induces a degeneration of the potential core with the appearance of vortices in the nozzle ejection vicinity which improves the jet diffusion. The effect of the acoustic excitation is pronounced in the jet initial region, which is squarely the most critical area for the technical devices that use the jet as a mixing device such as gas burners, we can affirm then that the acoustic excitation can be considered a useful methodology to obtain a rapid mixing with

a reduced length and also at a low turbulence level.

REFERENCES

Andersen, B. O., N. F. Nielsen and J. H. Walther (2016). Numerical and experimental study of pulse-jet cleaning in fabric filters. *Powder Technology* 291, 284–298

Binder G., M. Favre, V. Craya and H. TeVeug (1973). Jet Instationnaires. Labor de Mécanique des Fluides, Université de Grenoble.

Bremhorst, K. and W. H. Harch (1979). *Near Field Velocity Measurements in a Fully Pulsed. Subsonic Air Jet, Turbulent Shear Flows I*, Springer Verlag, Berlin, 37-54.

Chambers, F. W. and V. W. Goldschmidt (1982). Acoustic interaction with a turbulent plane jet effects on mean flow. *AIAA J.* 20, 797-804.

Crow, S. C. and Champagne F. H. (1971). Orderly Structure in Jet Turbulence. *Journal of Fluid Mechanics* 848, 547-591

Dimotakis, P. E. (2000). The mixing transition in turbulent flows. *Journal of Fluid Mechanics* 409, 69–98.

Farrington, R. B. and S. D. Claunch (1994). Infrared imaging of large-amplitude, low-frequency disturbances on a planar jet. *AIAA Journal* 32, 317-323.

Goldschmidt, V. W., M. K. Moallemi and J. W. Oler (1983). Structures and flow reversal in turbulent plane jets. *Physics of Fluids* 26, 428–432.

Goldschmidt, V. W. and K. F. Kaiser (1971). Interaction of an acoustic field and turbulent plane jet: mean flow measurements. *AICHE, Chem. Eng. Prod. Symp*. 109, 91-98.

Hariyo, P. S. and K. Bremhorst (2012). Experimental study on the propagation of a pulsed jet. *Procedia Engineering* 50, 174–187.

Hasan, M. A. Z. and A. K. M. F. Hussain (1982). The self-excited axisymmetric jet. *Journal of Fluid Mechanics* 115, 59-89.

Heskestad, G. (1965). Hot-wire measurements in a plane turbulent jet. *Journal of Applied Mechanics* 32, 721-734.

Hinze, J. O. (1987). Turbulence. McGraw-Hilleries in mechanical engineering. Ed. S.E. Mcgraw-Hill.

Ho, C. M. and L. S. Huang (1982). Subharmonics and vortex merging in mixing layers. *Journal of Fluid Mechanics* 119, 443-473.

Hsiao F. B., Lim Y. C., Huang J. M (2010). On the near-field flow structure and mode of behavior for the right-angle and sharp-edged plane orifice jet. Experimental Thermal and Fluid Science 34, 1282-1289.

Husain, H. S. and A. K. M. F. Hussain (1983). Controlled excitation of elliptic jets. *Letters of physics Fluids* 26, 2763-2766.

Hussain, F. and C. A. Thompson (1980). Controlled Symmetric Perturbation of the Plane Jet: An Experimental Study in Initial Region. *Journal of Fluid Mechanics* 100, 397-431.

Hussain, F. and H. S. Husain (1989). Elliptic jets. Part 1. Characteristics of unexcited and excited jets. *Journal of Fluid Mechanics* 208, 257–320.

Hussain, F. and K. B. M. Q. Zaman (1980). Vortex Pairing in Circular Jet Under Controlled Excitation. Part 2. Coherent Structure Dynamics. *Journal of Fluid Mechanics* 101, 493-544.

Kibens, V. (1980). Discrete Noise Spectrum Generated by an Acoustically Excited Jet. *AIAA J.* 18(4), 434-441.

Lio, S., H. Ken, Y. Katayama, Y. Haneda, T. Ikeda and T. Uchiyama (2013). Jet Flapping Control with Acoustic Excitation. *Journal of Flow Control, Measurement & Visualization* 1, 49-56.

Lovett, J. A. and S. R. Turns (1990). Experiments on axisymmetric pulsed turbulent jet flames. *AIAA Journal* 28(1), 38-46.

Marzouk, S., H. Ben Aissia and P. Georges Le (2015). Numerical study of amplitude and frequency effects upon a pulsating jet. *Computers and Fluids* 123, 99–111.

Rockwell, D. W. (1972). External Excitation of Planar Jets. *Journal of Applied Mechanics* 39, 883-890.

Sfeir, A. A. (1979). Investigation of three-dimensional turbulent rectangular jets. *AIAA J.* 17(10), 1055-1060**.**

Stamatios, P. L. and K. Ellen (2001). Asymmetric forcing of a turbulent rectangular jet with a piezoelectric actuator. *Physics of Fluids* 13(5), 1480-491

Tanaka, Y. (1984). On the Structure of Pulse Jet. *Bulletino f. J. S. M. E.* 230, 1667-1674.

Thomas, F. O. and V. W. Goldschmidt (1981). Interaction of an acoustic disturbance and a two dimensional turbulent jet: experimental data. *ASME Journal of Fluids Engineering* 105, 134-139.

Yeh, Y. L., Ch. Ch. Hsu, Ch. H. Chiang and F.B. Hsiao (2010). On the near-field flow structure and mode behaviors for the right-angle and sharp-edged orifice plane jet. *Experimental Thermal and Fluid Science* 34, 1282–1289.

Zaman, K. B. M. Q. and A. K. M. F. Hussain (1980). Vortex Pairing in a Circular Jet Under Controlled Excitation. Part 1. General Jet Response. *J. Fluid Mech*. 101, 449-491.